

Triple-Resonance Experiments for Correlation of H5 and Exchangeable Pyrimidine Base Hydrogens in ^{13}C , ^{15}N -Labeled RNA

Jens Wöhnert, Ramadurai Ramachandran,¹ Matthias Görlach, and Larry R. Brown

Abteilung für Molekulare Biophysik/NMR-Spektroskopie, Institut für Molekulare Biotechnologie e.V., Postfach 100813, D-07708 Jena, Germany

Received February 9, 1999; revised April 27, 1999

Triple-resonance two-dimensional H5(C5C4N)H experiments are described that provide through-bond H5 to imino/amino connectivities in uridines and cytidines in ^{13}C , ^{15}N -labeled RNAs. The experiments employ selective INEPT steps for transferring magnetization from the H5 hydrogens through the intervening C5, C4, and N3/N4 nuclei to the imino/amino hydrogens. The improved sensitivity of these experiments for assignments in a large 43-nucleotide RNA is demonstrated. © 1999 Academic Press

Key Words: RNA; heteronuclear NMR; assignment; isotope label; pyrimidine.

INTRODUCTION

Sequence-specific resonance assignment is the critical first step in the elucidation of biomolecular structures via NMR spectroscopy. Thus, in the case of isotope-labeled RNA, a variety of double- and triple-resonance experiments have been proposed to identify individual sugar and base spin systems, to link ribose anomeric hydrogens to the base H6/H8 hydrogens, and to achieve sequential resonance assignments of all nonexchangeable hydrogens (1, 2). The assignment of the exchangeable hydrogens is normally done independently of the assignment of the base and sugar hydrogens by the use of imino-imino/imino-amino sequential or intrabasepair nuclear Overhauser effects (NOEs) (3). In nonhelical regions such as bulges and loops this approach is no longer reliable since NOEs may arise from nonsequential spatial proximity. Recently novel triple resonance pulse sequences have been developed to provide through bond connectivities between the nonexchangeable and exchangeable hydrogens of a base, thereby extending the sequential assignments of the nonexchangeable hydrogens to the imino/amino hydrogens (4–8).

For linking of aromatic to imino/amino hydrogens in pyrimidine bases, different schemes have been proposed by Simorre *et al.* (4) and Sklenar *et al.* (5). The method of Simorre *et al.* achieves this correlation starting from the imino/amino hydrogens of uridines and cytidines and by making use of the two large one-bond scalar couplings J_{C4C5} , J_{C5C6} and the smaller

one-bond coupling $J_{\text{N3C4}}/J_{\text{N4C4}}$, whereas the latter approach employs three smaller one-bond CN-heteronuclear couplings for linking uridine H6 to the imino hydrogens. In experiments with a RNA molecule of 43 nucleotides, we had difficulty recording good correlation intensities with either of these experiments, probably as a consequence of adverse T_2 relaxation in a molecule of this size. To facilitate such correlations for larger RNA molecules, we propose here two new optimized pulse schemes for the use of a shorter coherence transfer pathway which correlates the H5 protons to the imino/amino protons of the pyrimidine bases. The efficiency of these experiments is demonstrated by presentation of spectral data recorded with a doubly labeled 43-nucleotide RNA derived from *Escherichia coli* 5S rRNA.

DESCRIPTION OF PULSE SEQUENCES

The magnetization transfer pathways involved in our approach are shown in Fig. 1 and the corresponding pulse sequences for achieving the chemical shift correlations in uridines and cytidines are shown in Figs. 2A and 2B. Since the ^1H chemical shift of pyrimidine H5 hydrogens is normally close to the water resonance, their chemical shifts are measured in the indirect dimension. The overall spectral width covered by the H5 hydrogens is limited and good spectral resolution can therefore be obtained with a limited number of t_1 increments. Starting from the H5 hydrogens, the magnetization is relayed through a series of INEPT transfer steps (9) to the imino/amino hydrogens. The H5 transverse magnetization created with the first 90° hydrogen pulse is frequency labeled during the evolution period t_1 and subsequently transferred to the attached C5 nucleus. The antiphase C5 carbon magnetization ($\text{C5}_x\text{H}_z$) evolves during period 2τ due to the C5–C4 scalar coupling while simultaneously becoming in phase with respect to the attached hydrogen ($\text{C5}_x\text{C4}_z$). To minimize the leakage of the C5 magnetization to the unwanted pathway involving the C6 carbon, the C5–C4 magnetization transfer employs band selective 180° pulses. The selective 180° pulse applied on the C4 is cosine modulated to minimize C5 resonance phase shifts (10) due to the Bloch–Siegert effect. At point b in the sequence, the C4 magnetization is antiphase with respect to the C5 carbon

¹ To whom correspondence should be addressed. Fax: 49–3641–656225. E-mail: raman@imb-jena.de.

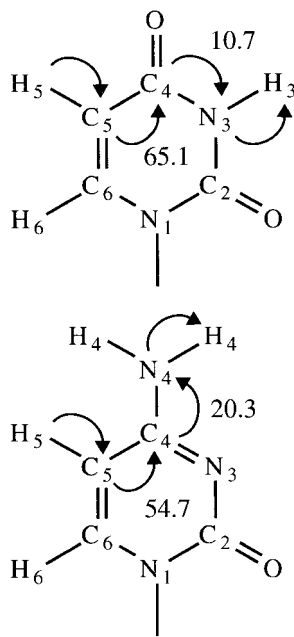


FIG. 1. Uridine (top) and cytidine (bottom) coherence transfer pathways employed for chemical shift correlation of the exchangeable and nonexchangeable hydrogens in the triple resonance 2D H5(C5C4N)H experiments. The C–N and C–C coupling constants ($2J$) used in the different coherence transfer pathways are indicated.

(C4_xC5_z). The C4 antiphase magnetization is then refocused with respect to the C5–C4 coupling and simultaneously evolves for a period of 2Δ to generate the C4_xN3_z/C4_xN4_z antiphase magnetizations in the case of uridines and cytidines, respectively. The phase shifts in the C4 resonances caused by the 180° pulse on C5 due to the Bloch–Siegert effect is compensated by a second 180° pulse on C5 at the end of the delay 2Δ . In the case of the cytidine optimized sequence (Fig. 2B), a selective 180° pulse on N4 is used to avoid the unwanted transfer of magnetization through the C4–N3 scalar interaction to the N3 spins. At point c in the sequence the ¹⁵N magnetization is antiphase with respect to the C4 carbon (N3_xC4_z/N4_xC4_z). During the next interval 2Δ this magnetization is refocused with respect to the C4–N3/C4–N4 coupling and allowed to evolve due to the N3–H3/N4–H4 coupling so as to lead to the formation of N3_xH3_z/N4_xH4_z at point d. To take into account the different number of ¹⁵N attached hydrogens in the case of uridines and cytidines, the time for the evolution due to the N–H scalar coupling is set to different durations in the two cases. In the case of the uridine optimized sequence, a selective 180° pulse on C4 is used to avoid leakage of magnetization through the unwanted N3–C2 pathway. The antiphase H3_xN3_z/H4_xN4_z magnetization obtained at point e is converted into an observable, in-phase hydrogen magnetization by the last refocusing step. To achieve water suppression the WATERGATE technique (11) is employed during this last step. Since the dispersion of the hydrogen chemical shifts in the regions of the H5 and imino/amino resonances may be

limited, especially in the case of the cytidines, the 2D H5(C5C4N)H experiment could be extended into a 3D H5(C5C4)NH experiment by converting the second delay 2Δ

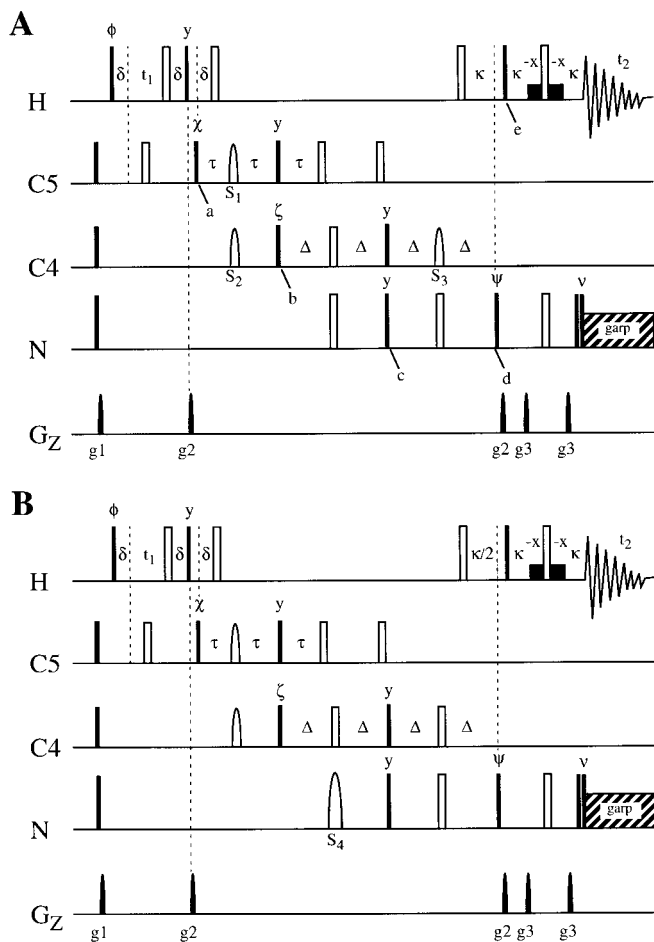


FIG. 2. Pulse sequences for the chemical shift correlation of (A) the imino and H5 hydrogens in uridine and (B) the amino and H5 hydrogens in cytidine in the H5(C5C4N)H experiments. Filled and open rectangles indicate 90° and 180° pulses, respectively. The power levels of the rectangular 90° and 180° pulses applied on C4 are adjusted so as to minimize the excitation of the C5 nuclei and vice versa (i.e., a 2.5-kHz RF field for 150.9-MHz ¹³C frequency). The hydrogen carrier is kept at the water frequency. The ¹³C5, ¹³C4, and ¹⁵N carriers are set to 105, 169, and 160 ppm in (A) and to 99, 168, and 100 ppm in (B), respectively. The selective 180° pulse S1 on C5 is an 814- μ s RE-BURP pulse (24) with an excitation bandwidth of 6.0 kHz. The selective 180° pulses S2 and S3 on C4 are I-BURP-2 pulses (24) with a duration of 1550 μ s and an excitation bandwidth of 3.0 kHz. Additionally, the S2 pulse is cosine modulated for minimizing Bloch–Siegert effects on C5 (10). In (B) a 1200- μ s RE-BURP (24) 180° pulse (S4) with an excitation bandwidth of 4000 Hz is used to achieve a selective transfer of magnetization from C4 to N4. The transfer delays employed were $\delta = 1.25$ ms, $\tau = 3.4$ ms, $\Delta = 10$ ms, and $\kappa = 2.5$ ms. The WATERGATE technique (11) is applied during the ¹⁵N–¹H INEPT step, using typically 1500- μ s selective 90° pulses flanking the nonselective 180° pulse. G1 to G3 denote the z-axis pulsed-field gradients employed. Unless otherwise specified, the pulses have phase = x . The phase cycle is $\phi = 8^*(x)$, $8^*(-x)$; $\chi = y, -y$; $\zeta = 16^*(y)$, $16^*(-y)$; $\psi = y, y, -y, -y$; $\nu = 4^*(x)$, $4^*(-x)$; receiver = $2^*(x, -x, -x, x)$, $4^*(-x, x, x, -x)$, $2^*(x, -x, -x, x)$. In addition, the phase ϕ was incremented according to the hypercomplex method (25) to obtain quadrature detection in t_1 .

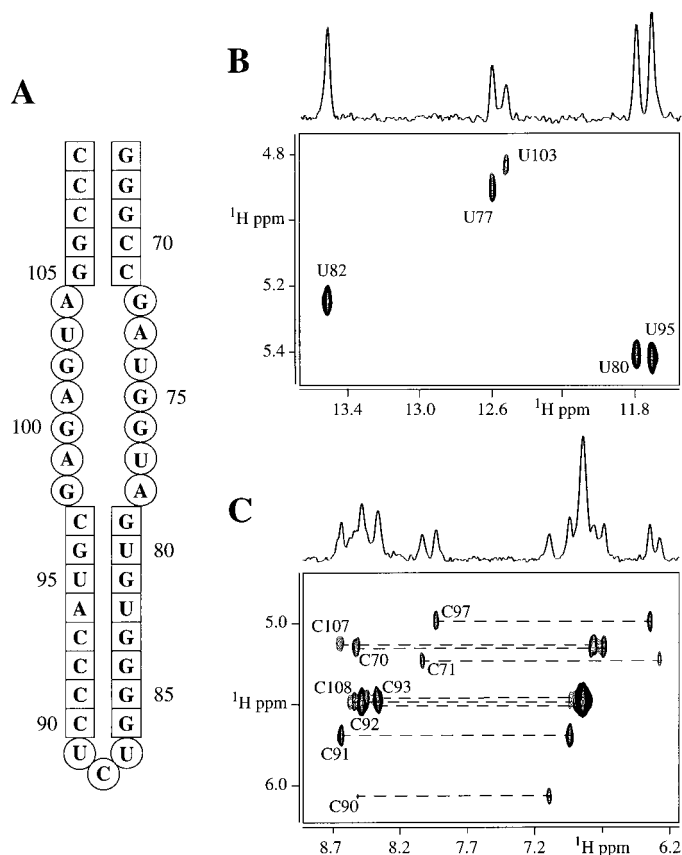


FIG. 3. (A) Secondary structure of the 43-nucleotide DE domain of 5S rRNA of *E. coli*. (B) Two-dimensional H5(C5C4N)H spectrum showing the cross-peaks between the uridine imino and uridine H5 resonances with the assignments indicated. The spectrum was acquired with 64×1024 complex points in t_1 and t_2 , respectively, spectral widths of 2000 Hz in F1 and 13,000 Hz in F2, 64 scans per t_1 increment, and a relaxation delay of 2 s. (C) Two-dimensional H5(C5C4N)H spectrum showing the cross-peaks between the cytidine amino and cytidine H5 resonances with the assignments indicated. Resonances belonging to the same amino group are connected by a dotted line. The spectrum was acquired with 64×1024 complex points in t_1 and t_2 , respectively, spectral widths of 2000 Hz in F1 and 13,000 Hz in F2, 256 scans per t_1 increment, and a relaxation delay of 2 s. The experiments were performed on a 0.8 mM uniformly ¹³C,¹⁵N-labeled RNA sample at 25°C on a Varian Unity INOVA 600 MHz spectrometer.

into a constant-time (12) evolution period for N3/N4 chemical shift labeling.

RESULTS AND DISCUSSION

Figures 3B and 3C illustrate the chemical shift correlations achieved with the sequences for the uridines and cytidines in the uniformly ¹³C, ¹⁵N-labeled 43-nucleotide RNA shown in Fig. 3A. The sample was prepared by *in vitro* transcription with T7 RNA polymerase (13) and a linearized plasmid template using uniformly ¹³C, ¹⁵N-labeled nucleotides essentially as described previously (14–16). The NMR sample contained 0.8 mM RNA, 60 mM KCl, 5 mM potassium phosphate buffer,

and 6 mM CaCl₂ at pH 6.0 in a volume of 600 μl. The lengths of the transfer delays τ and Δ were optimized experimentally for this molecule to $\tau = 3.4$ and $\Delta = 10$ ms. These values represented the best compromise between the optimal theoretical value of $1/4J$ and the minimization of relaxation losses. Two of the eight uridines (U87, U89) are located in the apical loop of the molecule and their imino hydrogens are not observable even at low temperatures, presumably as a consequence of rapid exchange with solvent water. The imino hydrogen resonance of U74 is broadened by fast exchange with the solvent at 10°C and not observable at higher temperatures (17). In the 2D H5(C5C4N)H spectrum optimized for uridine and acquired in 5 h, correlations are observed between all of the remaining five uridine H5 and imino resonances. Since the signals of the cytidine amino hydrogens are broadened by rotational exchange and each cytidine H5 hydrogen is connected to two amino hydrogens the experiment optimized for cytidine required 20 h of measurement time. Correlations could be obtained for 9 of 11 cytidines. The amino hydrogens of the terminal C109 as well as C88 located in the apical loop are in fast exchange with the solvent and therefore not observable. Due to the helical nature of the molecule used in this study (17, 18), the sequential imino/amino assignments for uridines and cytidines could be unambiguously confirmed from either ¹H–¹H NOESY or ¹H–¹H–¹⁵N NOESY-HSQC spectra. The ¹H chemical shifts for the H5 hydrogens obtained in the two experiments were adequate to assign the corresponding signals in the ¹H–¹³C HSQC spectrum, even in cases where cytidine and uridine H5 hydrogens had very similar chemical shifts (U80 and C93, U82 and C71, respectively) due to the different resonance frequencies of the C5 (in contrast to the C6) carbons of cytidine and uridine. In this context it should be noted that the chemical shift dispersion in the H5 region is as good as that observed for the H6 region and the linking of H5 to H6 resonances is easily obtained separately by one of several very sensitive methods such as HCCH-COSY and NOESY.

The H5(C5C4N)H experiments are an efficient and sensitive approach to obtaining links between exchangeable and nonexchangeable pyrimidine base hydrogens in larger RNAs or RNA–protein complexes. The efficiency of the above experiments does depend on the performance of the band selective pulses employed to avoid the leakage of magnetization through the unwanted C5–C6, N3–C2 (uridines), and C4–N3 (cytidines) scalar interactions since the chemical shift separations between C4/C2 and C4/C6 are only 15 and 20 ppm, respectively. However, at 600 MHz the desired selective coherence transfers could be readily achieved. In principle, selective C–N transfers are also possible by a heteronuclear C–N TOCSY mixing scheme (19–21) as in (4, 5), but the use of selective INEPT transfer steps allows the concatenation of different refocusing and defocusing periods, thereby leading to a further reduction of the net transfer time. The heteronuclear TOCSY mixing also requires the application of long, high power RF irradiation [~ 90 ms, 1.9 kHz in (4)] on the ¹⁵N channel, which

may exceed the safe power limits of commercially available probes (e.g., 100 ms, 1 kHz in our HCN and HCNP probes). Furthermore, compared with the heteronuclear TOCSY based coherence transfer schemes, where the need for completion of cycles (or half-cycles) of the mixing sequences has to be taken into account, the INEPT approach allows for ready optimization of the transfer delays with respect to T_2 relaxation. In the present experiments, the use of a coherence transfer pathway requiring fewer transfer steps, i.e., removal of the C5–C6 transfer step, the concatenation of the INEPT steps and optimization of the INEPT delays to take into account T_2 relaxation allowed us to shorten the total fixed delays to ~ 55 ms. This reduction plus the use of selective pathways proved decisive in being able to record good correlations to the uridine/cytidine exchangeable imino/amino hydrogens for the present RNA molecule of 43 nucleotides.

ACKNOWLEDGMENTS

This work was supported by a grant from the Deutsche Forschungsgemeinschaft (Br 1487/2-3). J.W. is grateful to the Fonds der chemischen Industrie for financial support.

REFERENCES

1. S. S. Wijmenga and B. N. M. van Buuren, The use of NMR methods for conformational studies of nucleic acids, *Prog. Nucl. Magn. Reson. Spectrosc.* **32**, 287–387 (1998).
2. G. Varani, F. Aboul-Ela, and F. H. Allain, NMR investigation of RNA structure, *Prog. Nucl. Magn. Reson. Spectrosc.* **29**, 51–127 (1996).
3. S. S. Wijmenga, M. M. W. Mooren, and C. W. Hilbers, NMR of nucleic acids: From spectrum to structure, in "NMR of Macromolecules" (G. C. K. Roberts, Ed.), pp. 217–288, Oxford Univ. Press, Oxford (1993).
4. J. P. Simorre, G. A. Zimmermann, A. Pardi, B. T. Farmer II, and L. Mueller, Triple resonance HNCCCH experiments for correlating exchangeable and nonexchangeable cytidine and uridine base protons in RNA, *J. Biomol. NMR* **6**, 427–432 (1995).
5. V. Sklenar, T. Diekmann, S. E. Butcher, and J. Feigon, Through-bond correlation of imino and aromatic resonances in ^{13}C -, ^{15}N -labelled RNA via heteronuclear TOCSY, *J. Biomol. NMR* **7**, 83–87 (1996).
6. J. P. Simorre, G. R. Zimmermann, L. Mueller, and A. Pardi, Correlation of the guanosine exchangeable and nonexchangeable base protons in ^{13}C -, ^{15}N -labelled RNA with an HNC-TOCSY-CH experiment, *J. Biomol. NMR* **7**, 153–156 (1996).
7. R. Fiala, F. Jiang, and D. J. Patel, Direct correlation of exchangeable and nonexchangeable protons on purine bases in ^{13}C -, ^{15}N -labelled RNA using a HCCNH-TOCSY experiment, *J. Am. Chem. Soc.* **118**, 689–690 (1996).
8. J. P. Simorre, G. R. Zimmermann, L. Mueller, and A. Pardi, Triple-resonance experiments for assignments of adenine base resonances in ^{13}C -, ^{15}N -labelled RNA, *J. Am. Chem. Soc.* **118**, 5316–5317 (1996).
9. G. A. Morris and R. Freemann, Enhancement of nuclear magnetic resonance signals by polarization transfer, *J. Am. Chem. Soc.* **101**, 760–762 (1979).
10. M. A. McKoy, Selective refocusing of C_β scalar coupling during indirect evolution of heteronuclear single-quantum carbon coherences, *J. Magn. Reson. Ser. B* **107**, 270–273 (1995).
11. M. Piotto, V. Saudek, and V. Sklenar, Gradient-tailored excitation for single- quantum NMR spectroscopy of aqueous solutions, *J. Biomol. NMR* **6**, 661–665 (1992).
12. J. Santoro and G. C. King, A constant-time 2D overbroadening experiment for inverse correlation of isotopically enriched species, *J. Magn. Reson.* **97**, 202–207 (1992).
13. J. F. Milligan, D. R. Groebe, G. W. Witherell, and O. C. Uhlenbeck, Oligoribonucleotide synthesis using *T7* RNA polymerase and synthetic DNA templates, *Nucleic Acids. Res.* **15**, 8783–8798 (1987).
14. M. Stoldt, J. Wöhnert, M. Görlach, and L. R. Brown, The NMR structure of *Escherichia coli* ribosomal protein L25 shows homology to general stress proteins and glutamyl-tRNA synthetases, *EMBO J.* **17**, 6377–6384 (1998).
15. M. Grüne, M. Görlach, V. Soskic, S. Klussmann, R. Bald, J. P. Fürste, V. A. Erdmann, and L. R. Brown, Initial analysis of 750 MHz NMR spectra of selectively ^{15}N -G,U labelled *Escherichia coli* 5S rRNA, *FEBS Lett.* **385**, 114–118 (1996).
16. C. Sich, O. Ohlenschläger, R. Ramachandran, M. Görlach, and L. R. Brown, Structure of an RNA hairpin loop with a 5'-CGUUUCG-3' loop motif by heteronuclear NMR spectroscopy and distance geometry, *Biochemistry* **36**, 13989–14002.
17. A. Dallas and P. B. Moore, The loop E-loop D region of *Escherichia coli* 5S rRNA: The solution structure reveals an unusual loop that may be important for binding ribosomal proteins, *Structure* **5**, 1639–1653 (1997).
18. C. C. Corell, B. Freeborn, P. B. Moore, and T. A. Steitz, Metals, motifs and recognition in the crystal structure of a 5S rRNA domain, *Cell* **91**, 705–712 (1997).
19. L. Mueller and R. R. Ernst, Coherence transfer in the rotating frame: Application to heteronuclear cross-correlation spectroscopy, *Mol. Phys.* **38**, 963–992 (1979).
20. L. R. Brown and B. C. Sanctuary, Hetero-TOCSY experiments with WALTZ and DIPSI mixing sequences, *J. Magn. Reson.* **91**, 413–421 (1991).
21. M. Ernst, C. Griesinger, and R. R. Ernst, Optimized heteronuclear cross polarization in liquids, *Mol. Phys.* **74**, 219–252 (1991).
22. G. M. Clore and A. M. Gronenborn, Application of three- and four-dimensional heteronuclear NMR spectroscopy to protein structure determination, *Prog. Nucl. Magn. Reson. Spectrosc.* **23**, 43–92 (1991).
23. J. H. Ippel, S. S. Wijmenga, R. de Jong, H. A. Heus, C. W. Hilbers, E. de Vroom, A. van der Marel, and J. H. van Boom, Heteronuclear scalar couplings in the bases and sugar rings of nucleic acids: Their determination and application in assignment and conformational analysis, *Magn. Reson. Chem.* **34**, S156–S176 (1996).
24. H. Geen and R. Freemann, Band selective radiofrequency pulses, *J. Magn. Reson.* **93**, 93–141 (1991).
25. D. J. States, R. A. Haberkorn, D. J. Ruben, A two-dimensional nuclear Overhauser experiment with pure adsorption phase in four quadrants, *J. Magn. Reson.* **48**, 286–292 (1982).